Environmental Engineering and Management Journal

November 2020, Vol. 19, No. 11, 2039-2048
http://www.eemj.icpm.tuiasi.ro/; http://www.eemj.eu

"Gheorghe Asachi" Technical University of Iasi, Romania

BAND GAP TUNING OF ZINC OXIDE NANOPARTICLES BY THE ADDITION OF (1-4%) STRONTIUM. SYNTHESIS, CHARACTERIZATION OF THE CATALYST AND ITS USE FOR THE PHOTOCATALYTIC DEGRADATION OF ACID VIOLET-17 DYE IN AQUEOUS SOLUTION

Fazal Akbar Jan[1*], Rahat Ullah[1], Umar Shah[1], Muhammad Saleem[1], Naimat Ullah[2]

[1]Department of Chemistry, Bacha Khan University Chrasadda, Khyber-Pakhtunkhwa, 24420 Pakistan
[2]Department of Chemistry, Qauid-i- Azam University Islamabad, 45320 Pakistan

Abstract

Zinc oxide and strontium doped zinc oxide nanoparticles were synthesized through hydrothermal route. The synthesized nanoparticles were characterized by UV, FTIR, SEM, X-Ray diffraction (XRD) and energy dispersive x-ray (EDX) spectroscopic techniques. The optical band gaps were calculated to be 3.16EV and 2.90EV for ZnO and Sr-ZnO nanoparticles, respectively. FTIR confirmed the incorporation of the Sr into ZnO nanoparticles. Average particles size of undoped ZnO and Sr-doped ZnO nanoparticles was also calculated and found to be 16 nm and 21 nm, respectively. ZnO and Sr-doped ZnO nanoparticles were found to have spherical shape while in the last case, the particles were smaller in size and with more agglomeration. The synthesized nanoparticles were also applied as photo catalyst for the degradation of Acid violet- 17 dye in aqueous solution. The photo catalysis was performed both in UV-light and sun light irradiation. Undoped ZnO nanoparticles were found to have high photo catalytic activity as compared to its counterpart Sr-doped nanoparticles. The degradation rate of Acid violet- 17 was found to increase with increase in irradiation time, initial concentration of the dye and weight of catalyst. By increasing the pH of the medium, the rate of degradation also increased.

Key words: acid violet, band gap, catalytic degradation, EDS, nanoparticles, Sr-doped ZnO

Received: October, 2019; Revised final: January, 2020; Accepted: May, 2020; Published in final edited form: November, 2020

1. Introduction

It is a fact that industrialization and urbanization has deteriorated water quality and posed negative impacts on human health and other living organisms. Industrial effluents of most of the industries such as lather, textile, paper, cosmetics and printing contain organic dyes and pigments cause severe water problems (Salama et al., 2018). Among tons of dyes produced annually about 2% are discharged in effluent during manufacturing operations (Anwer et al., 2019; Kaur et al., 2015). During dying process only a portion of dye is fixed to the fabric and the rest is washed away which lead to an increase of dye concentration in the receiving water (Hassaan and El Nemr, 2017). The color produced in the receiving water due to the presence of dyes is persistent, stable, fast, toxic and inhibitory. The dyes are difficult to degrade and thus entail the receiving water to be inadequate for use. Biological and photosynthetic processes in the aquatic environment are affected by high concentrations of textile dyes (Yaseen and Scholz, 2018). Complex organic framework of dyes containing heavy metals can induce chronic toxicity which may be teratogenic, mutagenic and carcinogenic. Long term exposure to dyes can cause tumors, cancer and affect liver and kidney as reported by many investigations (Reddy et

* Author to whom all correspondence should be addressed: e-mail: fazal_akbarchem@yahoo.com

al., 2008). In order to meet water requirements for irrigation, recycling and reuse of water has become vital (Sarkheil et al., 2014). Governmental organizations and water industries are focused to develop cost-effective technologies for water/wastewater treatment and reclamation. A number of chemical and physical processes such as coagulation, reverse osmosis, ion exchange, ozonation, flocculation, activated carbon adsorption, Fenton process, advanced oxidation, electrochemical oxidation and photo catalysis have been reported for the removal of toxic substances from wastewater (Sarkar et al., 2017). Treating wastewater containing textile dyes by conventional chemical, physical and biological methods are associated high cost, generation of secondary pollutants and high energy requirement (Reza et al., 2017). On the other hand, photocatalytic degradation of dyes or other organic pollutants have attracted the attention of researchers in the 20th century (Viswanathan, 2018). Because of its cheapness, good catalytic activity, nontoxic nature, band gap of 3.37eV, binding energy of 60 mega-electron volts, ZnO is a semiconductor material and under ultraviolet- light has the ability to decompose many toxic compounds (Bagheri et al., 2020; Nagaraju et al., 2017; Pradyast et al., 2018). The incident light has the ability to generate photo-induced electron-hole pairs. Various chemical and physical properties including electronic structure, charge transport, optical and surface properties of ZnO are closely related to V_O (oxygen vacancies) which has been proved by many theoretical and experimental works. Isolated energy levels are created due to V_O, which significantly enhances the charge generation, optical absorption and separation (Kudo and Miseki, 2009).

The development of a wide band gap of ZnO is necessary for effective utilization of solar radiations and for this purpose alkaline earth metal can be used as dopants to regulate and control the band gap (Rekha et al., 2010; Wang et al., 2018; Yousefi et al., 2015). Keeping in view the importance of nanoparticles and the doping for decreasing the band gap a study was designed to synthesize bare ZnO and Sr-doped ZnO nanoparticles. The purpose of the present study was to compare the efficiencies of both doped and undoped ZnO nanoparticles for further use in degradation of selected dye in aqueous solution.

2. Material and methods

2.1. Reagents

All the chemical i.e. Zinc-acetate dihydrate ($Zn(CH_3CO_2)_2.2H_2O$), sodium hydroxide (NaOH), strontium chloride hexahydrate ($SrCl_2.6H_2O$), ethanol and Acid violet- 17dye were guaranteed chemicals purchased from Sigma Aldrich. Glass wares were washed with double distilled water to be free from any contamination.

2.2. Apparatus

UV-visible spectrophotometer Model Shimadzu UV-1800, Japan was used for all absorbance measurements. Perkin Elmer FTIR spectrometer version 10.4.00 was used for identification of the functional groups. For pH measurements, Elico (model IL-610) digital pH meter was used. All the analysis was performed in Advance Research Lab (ARL) Department of Chemistry Bacha Khan University Charsadda. SEM and EDS analysis of the synthesized materials were carried out in the Centralized Resource Laboratory (CRL) University of Peshawar.

2.3. Synthesis of nanoparticles

Zinc oxide nanoparticles were synthesized by the following hydrothermal method. Exactly 0.473 g zinc-acetate dihydrate was dissolved in 25 mL of ethanol. Then 1M solution of NaOH was prepared in distilled water. The NaOH solution was added to the salt solution drop wise until the pH reaches 10. For ensuring homogeneity, the solution was stirred for 10 minutes. Then the solution was transferred to an autoclave and placed in oven at temperature of 200°C for 6 hours. The product was filtered and washed several times with ethanol to neutralize the pH followed by drying at 800°C. For strontium doped zinc oxide, strontium chloride hexahydrate by weight percentage (1-4%) was dissolved before adding the zinc acetate dihydrate and the same method was repeated (Bharti and Bharati, 2016).

2.4. Preparation of dye

Stock solution (500ppm) of Acid violet- 17 dye was prepared by dissolving 0.125 gram of dry powder of dye in distilled water and was vigorously shaken. From stock solution, working solutions of different concentrations were prepared using the dilution formula (Eq. 1).

$$C_{M_1}V_1 = C_{M_2}V_2 \quad (1)$$

where: C_{M1} (ppm), V_1 (mL) is concentration and volume of the stock solution, C_{M2} (ppm), V_2 (mL) is the concentration and volume of the solution to be prepared.

2.5. Photocatalytic degradation of the dye

The catalytic activities of bare ZnO and Sr-doped ZnO nanoparticles were evaluated for applying them for the degradation of Acid violet- 17. For the assessment of enhanced activity, the photo catalytic degradation of the dye was carried out both in UV-light and sun light irradiation.

The wavelength of maximum absorption (λ_{max}) of AV- 17 was found at 546 nm and this was used as a monitor wavelength for photo degradation. An appropriate amount of the photo catalyst was separately added to the dye working solutions. The solution was stirred for 30 minutes in dark in order to establish adsorption/desorption equilibrium before the photo degradation reaction. The dispersions was kept under light source. During experiments UV-lamp with the power of 1500 watts was placed at 15 cm away from the surface of the solution in locally designed equipment. The dye degradation was checked at various intervals of time by removing a portion from the dispersion and the catalyst was removed by centrifugation. The same process was repeated in sun-light. The absorbance of centrifuged solution was measured via UV-Visible Spectrometer. The percentage photo degradation of AV 17 was calculated by using the following relation (Eq. 2).

$$D\% = \frac{C_o - C_1}{C_o} x100 \quad (2)$$

where: C_0 and C denotes the concentrations of AV -17 at time 0 and t (s), respectively, and t is the irradiation time.

3. Result and discussions

3.1. Characterization of the catalysts

3.1.1.UV-VIS studies

The UV-Vis spectra of undoped ZnO and Sr-doped ZnO nanoparticles are shown in Fig. 1. The spectrum (Fig. 1a) shows the maximum absorption peak at wavelengths of 365 nm.

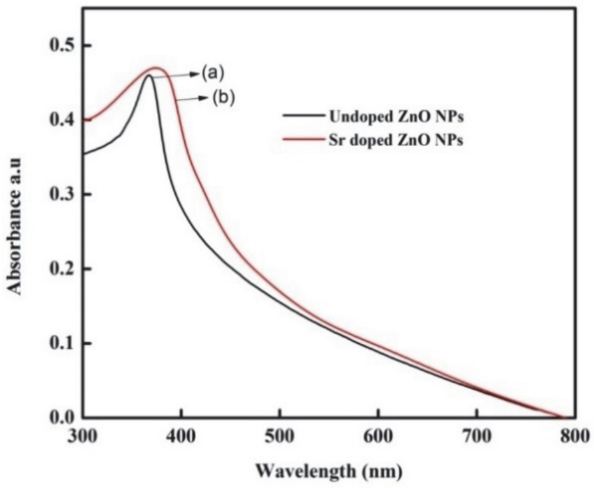

Fig. 1. UV-Vis spectra of: (a) Bare ZnO and (b) Sr-doped ZnO nanoparticles

The red shift in spectrum was observed due to strontium doping (376 nm) indicating bathochromic shift as compared to undoped ZnO nanoparticles (Perumal et al., 2015). The energy gaps were calculated from UV-Visible spectrum using the following relation (Eq. 3):

$$\alpha \cdot h \cdot v = A \cdot (h \cdot v \cdot E_g)^n \quad (3)$$

where: α = absorption coefficient; $h\upsilon$ = energy of photon; A= proportionality constant and n = the index.

The band gap of bare ZnO and Sr-doped ZnO nanoparticles calculated from UV-VIS study was 3.16eV and 2.90 eV, respectively as shown in Fig. 2.

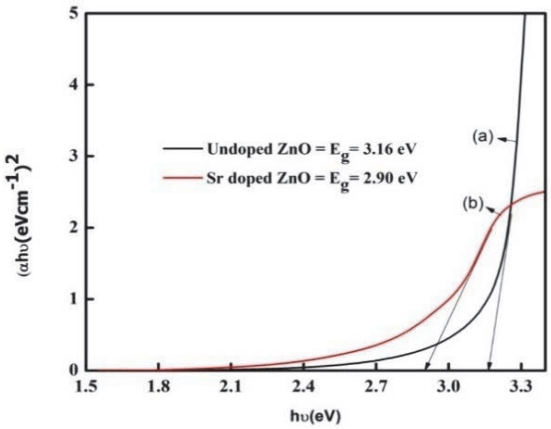

Fig. 2. Band gaps of (a) Bare ZnO and (b) Sr-doped ZnO nanoparticles

3.1.2. FTIR studies

Figs. 3a and b shows FTIR spectra of bare and Sr-doped ZnO nanoparticles. A broad peak at 3355 cm^{-1} corresponds to O-H stretching mood of the hydroxyl group, this is because of zinc hydroxide preserve some adsorbed water on its surface.

The bands between 1700-1000cm^{-1} corresponds to organic traces (residue) present in nanoparticles (Fig. 3a). The characteristic peak between 900-400 cm^{-1} correspond to Zn-O stretching mode (Xiong et al., 2006). In case of Sr doped ZnO (Fig. 3b), the peaks shifting and the new peak appearance at 469 cm^{-1} indicate Sr-O bonding which confirms the successful doping (Shanthi et al., 2018).

3.1.3. XRD studies

Figs. 4a-b shows powder XRD patterns of bare ZnO and Sr-doped ZnO nanoparticles. This was carried out to observe its crystallinity, size and structure of particles. There are seven peaks in the XRD pattern. ZnO nanoparticles appearing at 2 thetas of 31.72°, 34.34°, 36.14°, 47.46°, 56.47°, 62.78°, and 69°. Synthesized ZnO nanoparticles according to JCPSD card No 01-079-2205, confirming the hexagonal wurtzite structure (Kumar and Pandey, 2017). In case of strontium doping all the ZnO peaks were observed in XRD pattern of Sr-doped ZnO nanoparticles as shown in Fig. 4b.

There are small ignorable peaks shifting and decreasing the intensity of the major peaks of ZnO in Sr-doped ZnO pattern confirming that Sr is successfully doped into ZnO (Yousefi et al., 2015). Average particles size (Table 1) of undoped ZnO and Sr-doped ZnO nanoparticles were also calculated which comes out to be 16 nm and 21 nm, respectively

from XRD data using Debye Scherer equation (Eq. 4) (Perumal et al., 2015).

$$D = \frac{K\lambda}{\beta \cos \theta} \quad (4)$$

where: D is the average particle size; K is a dimensionless shape factor; λ is the X-ray wavelength; β is the line broadening at half the maximum intensity; Θ is the Bragg angle.

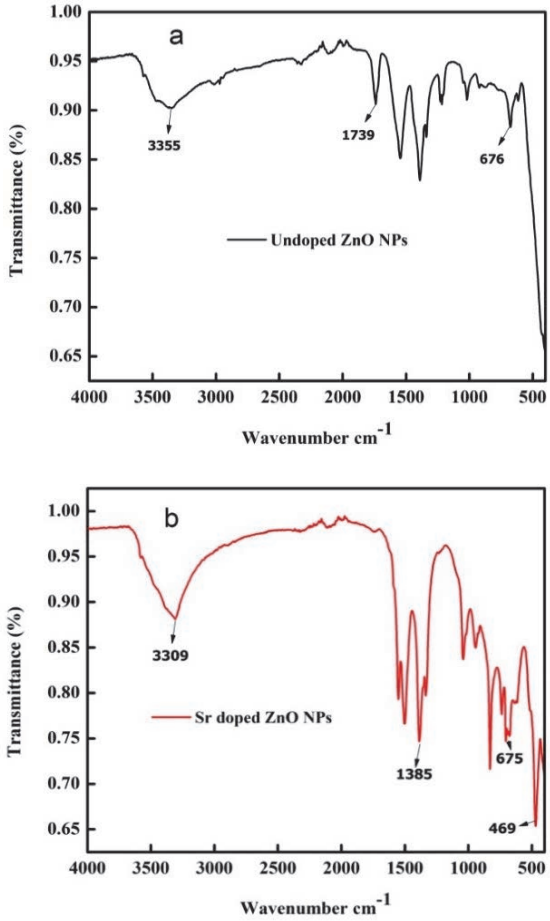

Fig. 3. FTIR spectra of (a) undoped ZnO (b) Sr doped ZnO

3.1.4. SEM studies

Figs. 5a and b shows SEM images of bare ZnO and Sr-doped ZnO nanoparticles obtained at 200 nm magnifications. It is evident from the images that ZnO have spherical shape with agglomeration which is attributed to the surface reactivity of ZnO (Fig. 5a). In case of Sr doped ZnO nanoparticles (Fig. 5b), the particles have smaller spherical shape as compared to undoped ZnO NPs and was found to be in more agglomeration (Shanthi et al., 2018). The obvious increase in agglomeration can also lead to decrease photo catalytic ability of the NPs.

3.1.5. EDX studies

Energy Dispersive X-rays spectroscopy was used for finding the elemental composition of undoped ZnO and Sr-doped nanoparticles as shown in Figs. 6a-b. The EDX spectra indicate the presence of ZnO and Sr as major elements and give the quantitative measurement of weight percentage of compositional elements (Raj et al., 2016). The weight percentage and elemental composition of the elements are summarized in Table 1.

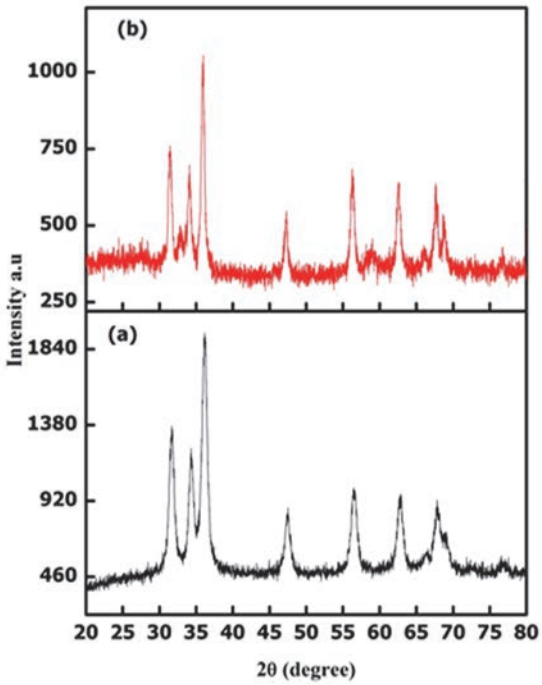

Fig. 4. XRD patterns of (a) undoped ZnO and (b) Sr doped ZnO

3.2. Effect of irradiation time on the photo catalytic degradation of dye

The photo catalytic degradation of Acid voilet-17 was carried out both in UV-light and sun light irradiation. The degradation was carried out at various interval of time ranging from 20 to 140 minutes. The aqueous solution of the dye was kept in light source after adding 0.01g of catalyst. A portion of the dispersion was taken out at the time interval of 20 minutes each and analyzed using UV Visible spectrophotometer.

The rate of dye degradation increased with the increase in time duration. At the initial 20 minutes time interval 34% and 9.96% (Figs. 7a-b) of dye was degraded using ZnO and Sr-doped ZnO nanoparticles, respectively which increased to 85 % and 78 % at 140 minutes interval. The percent degradation achieved at different intervals of time is briefly described in Table 2. The same process was repeated in sun light keeping all other parameters constant. At the initial 20 minutes time interval about 43% and 14.2% degradation of Acid violet-17 was observed. Again, with increase in time duration, the rate of degradation increased and reached 94% and 88% at 140 minutes using both undoped and doped catalysts, respectively (Figs. 8a-b). The percent degradation achieved at different interval of time is briefly described in Table 3. Best degradation was noticed while using sun light so the remaining experiments were carried out under the sun light.

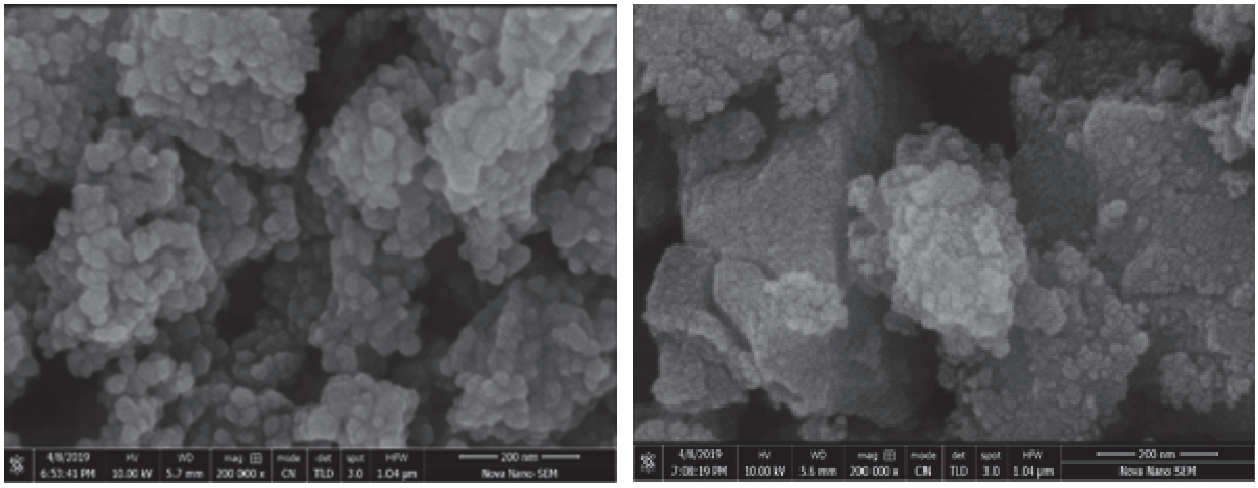

Fig. 5. SEM photographs of (a) undoped ZnO and (b) Sr doped ZnO

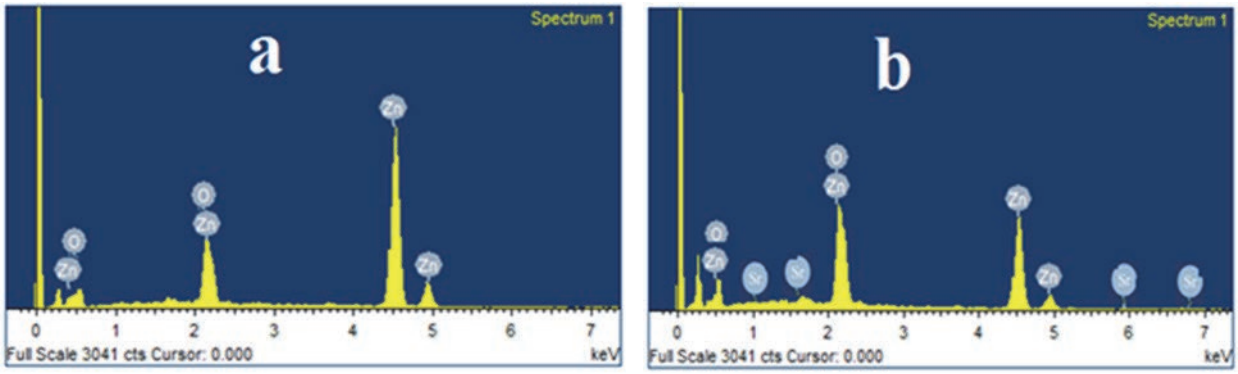

Fig. 6. Energy dispersive X-rays spectra of (a) undoped ZnO (b) Sr doped ZnO

Table 1. EDX elemental composition of undoped ZnO and Sr-doped ZnO nanoparticles

S.No	***Samples***	***wt%O***	***wt%Zn***	***wt%Sr (dopant)***
1	Undoped ZnO	51.25	48.75	--
2	Sr doped ZnO	61.81	37.02	1.18

Table 2. Increase in percent degradation of the dye with increase in time using undoped ZnO and Sr-doped ZnO nanoparticles in UV light

Time (mints)	20	40	60	80	100	120	140
Degradation (%) ZnO	34	53	59	66	74	77	85
Degradation (%) Sr-ZnO	9.96	19	31	43	56	69	78

Table 3. Increase in percent degradation of the dye with increase in time using undoped ZnO and Sr -doped ZnO nanoparticles in sun light

Time (mints)	20	40	60	80	100	120	140
Degradation (%) ZnO	43	48	64	79	84	87	94
Degradation (%) Sr-ZnO	14.2	27	42	46	62	69	88

Two things were observed. First of all we observed that the photo catalyst showed high activity at the initial time and slightly decreased with increasing of time. This can be attributed to the fact that initially the photo catalyst surface is exposed to more light photons. With increase of time duration, the catalyst surface is saturated by the dye molecules. As a result, the concentration of OH• which are needed for the degradation of dye molecules decreases and thus, the photo catalyst activity is suppressed. Secondly, the degradation process was effective in sun light as compared to UV-light. This is because the sun light heat up the dye solution and thus speed up the photo catalytic process.

Literature shown that when reaction temperature increases the photo catalytic process is enhanced. When the temperature of reaction is below 80 °C it favors the adsorption while when is further reduces to 0 °C, activation energy increased noticeably (Mamba et al., 2014).

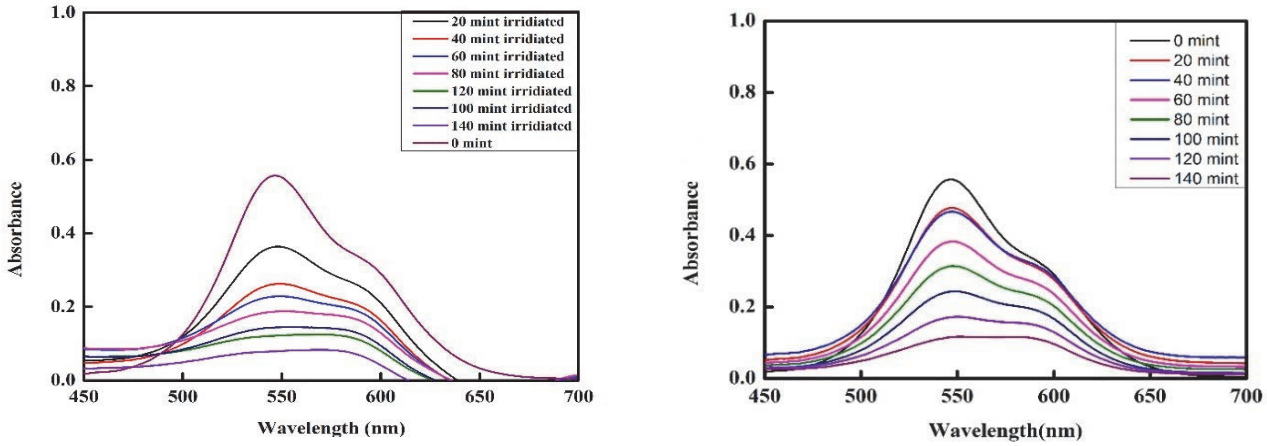

(a) (b)

Fig. 7. Effect of time on the degradation of dye using (a) undoped ZnO (b)Sr-doped ZnO in UV light

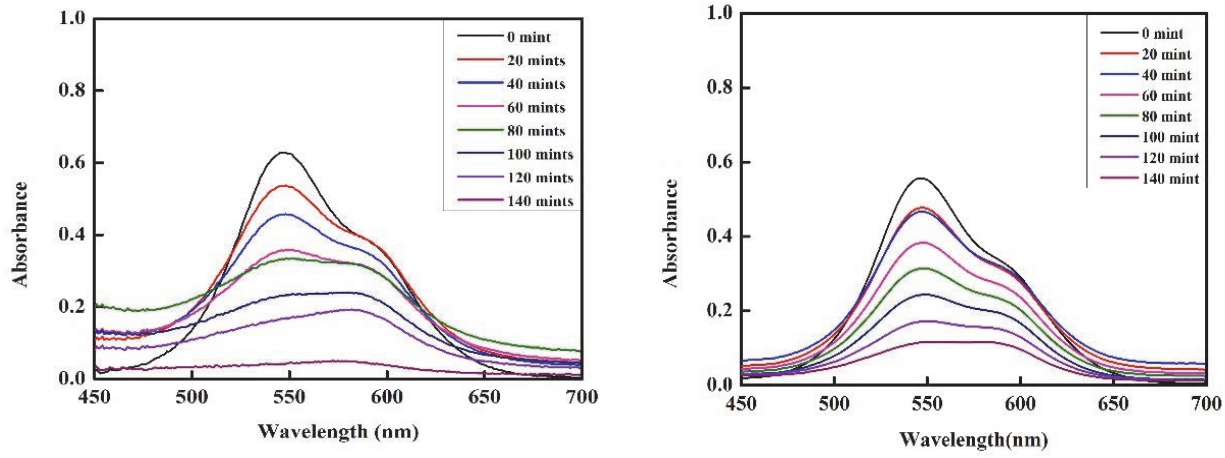

(a) (b)

Fig. 8. Effect of time on the degradation of dye using (a)undoped ZnO; (b) Sr-doped ZnO in sun light

A temperature range of 20-80 °C has been regarded as an effective for photo mineralization of organic content. For tuning of the band gap of the pure ZnO NPs, Sr was used as dopant. The catalytic activity of ZnO NPs increases with the decrease in the band gap. It is due to the fact that when the band gap decreases the electron can easily excite to the conduction band and large number of electron and hole pairs are generated which result in the formation of more radicals but in this case the band gap decreases to such a value that now electrons and hole pair recombination increases.

That is why doped ZnO has less catalytic activity as compared to its counterpart. Moreover, when Sr was added as a dopant, the penetration depth of light into ZnO enhance the space charge layer which lowers the photo catalytic activity by the recombination of generated electron hole pairs. Besides this, the dopant also covers the surface of ZnO and hence lowers the activity (Dodd et al., 2009; Khataee et al., 2015; Salvi et al., 2016).

3.3. Effect of dye concentration on degradation

On photo catalysis process the effect of initial dye concentration was evaluated using different concentrations ranging from 5-30 ppm and keeping the amount of catalyst constant. The experimental results revealed that the percent degradation of AV-17 decreases with increase in initial concentration. Table 4 shows the percent degradation of the dye achieved using various concentrations of the dye. As evident from Figs. 9a-b, the catalyst surface from light photons is shielded due to the adsorption of more dye molecules as a result of the increase in the initial dye concentration (Daneshvar et al., 2003; Saggioro et al., 2011). This can also be attributed to the fact that increase in the dye concentration saturate the photo catalyst surface and the requirement of catalyst for the process also increases. Keeping the irradiation time and catalyst loading constant, the $OH^{\cdot}$ radical formation on the surface of semiconductor also become constant. That is why increasing concentration of the dye the relative number of OH•

needed for the dye molecules decreases (Mengyue et al., 1995). For photo catalytic process, lower concentration of the dye was found to be more effective.

3.4. Effect of catalyst dosage

To obtain an effective photo catalytic degradation the catalyst dosage is an important parameter. Increasing the amount of catalyst will increase active sites which in turn increase the number of superoxide and hydroxyl radicals (Daneshvar et al., 2004). To know about the effect catalyst dosage on the degradation efficiency a 10ppm solution of AV-17 dye was used while adding ZnO and Sr -doped ZnO of varying weight (0.01 – 0.07g). The process was carried out under sun light irradiation. The time duration of 80 minutes was found to be an optimum time. Using 0.01g, 0.02g, 0.03g and 0.04g of pure ZnO catalyst about 91%, 91%, 92.5% and respectively 93% percent degradation was found (Figs. 10a and b). Increasing the amount of catalyst up to 0.05g-0.07g, the degradation decreased to 91%, 88% and 72%, respectively. In case of Sr-doped ZnO, the degradation observed using 0.01g, 0.02g, 0.03g, 0.04g and 0.05g of the catalyst was 59%, 61 %, 72%, 72% and 92%, respectively. Increasing the amount of catalyst from 0.06 to 0.07g, the percent degradation noted was 74% and 59.5 %, respectively. Among the different catalyst loadings, higher degradation rate was achieved with 0.04g of undoped ZnO and 0.05g of Sr-doped ZnO nanoparticles. With further increase in the amount of the catalyst, the degradation rate substantially decreased. This can be attributed to the shielding of the photons by the suspension (Akpan and Hameed, 2009). For the degradation of a dye in wastewater an optimum amount of the catalyst should be used above which the rate of degradation will eventually decreases. It has been reported that the maximum dosage of the photo catalyst for maximum activity is 3-4 g per liter of the dye solution (Viswanathan, 2018).

3.5. Effect of pH of the solution

Initially the pH of the dye solution was 6.1. The pH range of 4-9 was adjusted during experiments in order to study the effect of initial pH on the degradation efficiency of pure ZnO and Sr-doped ZnO catalysts. The photo catalytic activity of both catalysts was observed to be significantly affected by the pH. Using ZnO, the degradation rate increased from 71% to 88% as the pH was increased from 4 to 9 as shown in Fig. 11a, while for Sr-doped ZnO the degradation activity rise from 59% to 94% as shown in Fig.11b. The percent degradation achieved at different pH is briefly presented in Table 5.

For the photo catalytic degradation process adsorption of dye is an essential step. The dye which has high adsorption capacity will degrade faster. Higher concentration of hydroxyl ions is provided at higher pH in order to react with holes on the ZnO and to form hydroxyl radicals which subsequently causes an improved photo catalytic degradation. The concentration of hydroxyl radicals and adsorption on photo catalyst will determine the extent of degradation (Li et al., 2011). Activity of ions (e.g. H+ or pH) determines the potential of the surface charge in photo catalyst/aqueous systems.

Table 4. Percent degradation of the dye using different concentration of undoped ZnO and Sr -doped ZnO nanoparticles in sun light

Concentration (ppm)	***5ppm***	***10 ppm***	***15 ppm***	***20 ppm***	***25 ppm***	***30 ppm***
Degradation (%) ZnO	93	75	72	67	51	19
Degradation (%) Sr-ZnO	85	58	45	35	25	13

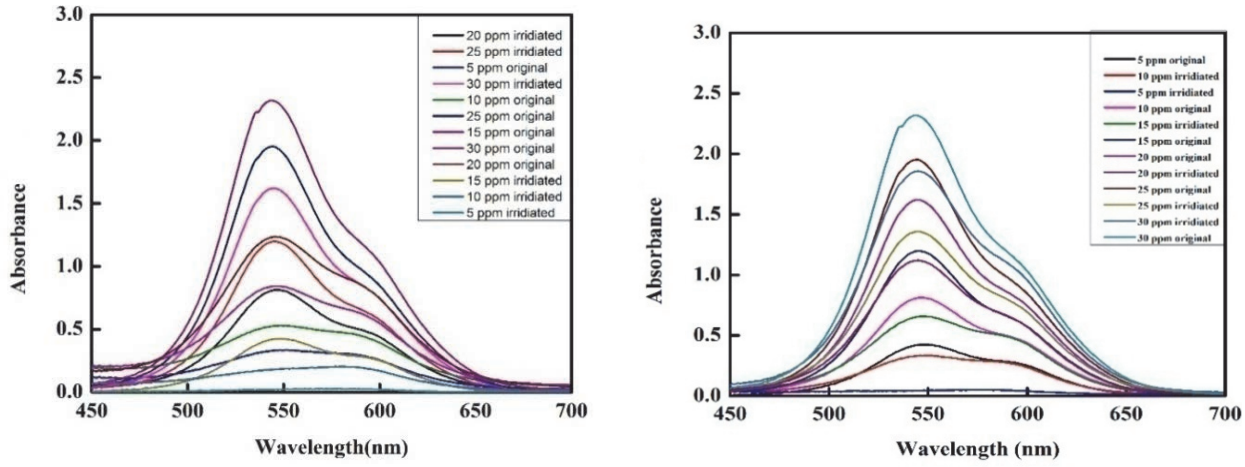

(a) (b)

Fig. 9. Effect of concentration on the degradation of dye using (a) undoped ZnO (b) Sr-doped ZnO in sun light

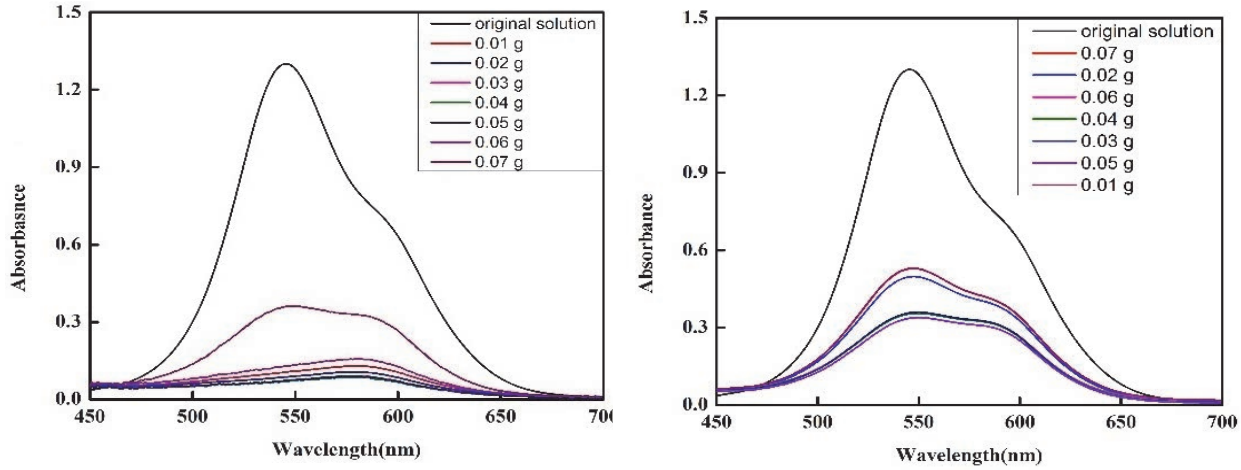

(a) (b)

Fig. 10. Effect of catalyst dosage on the degradation of dye using (a)undoped ZnO (b) Sr-doped ZnO in sun light

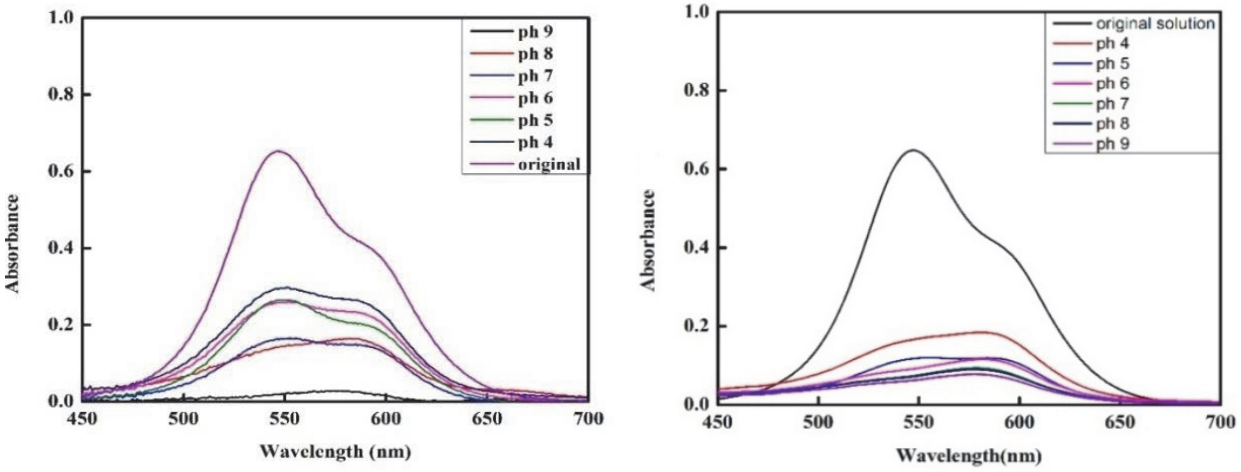

(a) (b)

Fig. 11. Effect of pH on the degradation of dye using (a) undoped ZnO; (b) Sr-doped ZnO in sun light

Table 5. Percent degradation achieved at different pH value using ZnO and Sr-doped ZnO

pH value	4	5	6	7	8	9
Percent degradation (ZnO)	71%	81%	85%	86%	86%	88%
Percent degradation (Sr-ZnO)	54 %	59 %	60 %	74 %	74 %	95 %

The property of a surface to become either positively or negatively charged is a function of pH (Zhang et al., 1998). Maximum degradation of AV-17 was observed in basic medium in our study. Photo generation of •OH radicals is facilitated by the excess of hydroxyl anions in alkaline mediums which acts as a primary oxidizing agent responsible for photo catalytic degradation (Elaziouti and Ahmed, 2011).

3.6. Proposed mechanism for the photocatalytic effect of Sr-ZnO catalyst

Upon absorption of UV light by Sr-doped ZnO nanoparticles, an electron from valence band (VB) get excited to the conduction band (CB). As shown in Eq. (5) a positively charged hole in the valence band (hvb^+) and negative charge in the conduction band (ecb^-) are created. The H_2O molecules interact with the valence band holes forming OH• radicals (Eq. 6).

The reactive $OH^•$ radicals attack on dye molecule successively to make degradation. $O_2•^-$ (superoxide radical anion) are created by the interaction of electrons present in the conduction band ecb^- with the dissolved O_2 as shown in Eq. (7).The hvb^+ holes in the valence band thus created can interact with donor $HO_2^•$ and produce $OH^•$ radical. This will further attack the dye (Eq. 8).

$$Sr/ZnO + hv \rightarrow ecb^- + hvb^+ \quad (5)$$

$$H_2O \rightarrow H^+ + OH^- + hvb^+ \rightarrow H^+ + {}^•OH \quad (6)$$

$$O_2 + ecb+ \rightarrow O2^{•-} + H^+ + OH^- \rightarrow HO_2^• + {}^-OH \quad (7)$$

$$HO_2^{\bullet} + {}^{-}OH + hvb^{+} \rightarrow OH^{\bullet} \quad (8)$$

4. Conclusions

Sr doped ZnO nanoparticles are smaller in size, spherical and more agglomerated as compared to pure ZnO NPs. Average particle size of bare ZnO and Sr-doped ZnO was found to be 16 nm and 21 nm, respectively. The optical band gaps of bare ZnO and Sr-ZnO was 3.16 E_V and 2.90E_V, respectively.

The band gap of doped nanoparticles is sharp compared to undoped form, but still has low photo catalytic activity. This can be attributed to fact that the band gap decreases to such a value that now electron and hole pair recombination increases. That is why doped ZnO has less catalytic activity as compared to its counterpart.

Moreover, when Sr was added as a dopant then the penetration depth of light into ZnO enhance the space charge layer which lowers the photo catalytic activity by the recombination of generated electron hole pairs. Besides this, the dopant also covers the surface of ZnO and hence lowers the activity. In the sun light both catalysts showed enhanced photo catalytic activity as compared to UV light. The increase in pH of the medium linearly increased the percent degradation of Acid voilet-17.

References

Akpan U.G., Hameed B.H., (2009), Parameters affecting the photocatalytic degradation of dyes using TiO_2-based photo catalysts: A review, *Journal of Hazardous Materials*, **170**, 520-529.

Anwer H., Mahmood A., Lee J., Kim K.H., Park J.W., Yip A.C., (2019), Photo catalysts for degradation of dyes in industrial effluents: Opportunities and challenges, *Nanomaterials Research*, **12**, 955-972.

Bharti D.B., Bharati A.V., (2016), Synthesis of ZnO nanoparticles using a hydrothermal method and a study its optical activity, *The Journal of Biological and Chemical Luminescence*, **32**, 317-320.

Bagheri M., Najafabadi N.R., Borna E., (2020), Removal of reactive blue 203 dye photo catalytic using ZnO nanoparticles stabilized on functionalized MWCNTs, *Journal of King Saud University of Sciences*, **32**, 799-804.

Daneshvar N., Salari D., Khataee A.R., (2004), Photocatalytic degradation of azo dye acid red 14 in water on ZnO as an alternative catalyst to TiO_2, *Journal of Photochemistry and Photobiology A*, **162**, 317-322.

Daneshvar N., Salari D., Khataee A.R., (2003), Photocatalytic degradation of azo dye acid red 14 in water: investigation of the effect of operational parameters, *Journal of Chemical Technology and Biotechnology*, **157**, 111-116.

Dodd A., McKinley A., Tsuzuki T., Saunders M., (2009), Tailoring the photocatalytic activity of nanoparticulate zinc oxide by transition metal oxide doping, *Material Chemistry and Physics*, **114**, 382-386.

Elaziouti A., Ahmed B., (2011), ZnO-assisted photocatalytic degradation of Congo Red and Benzopurpurine 4B in aqueous solution, *Journal of Chemical Engineering Process and Technology*, **2**, 1-9.

Hassaan M.A., El Nemr A., (2017), Health and environmental impacts of dyes: mini review, *American Journal of Environmental Science and Engineering*, **1**, 64-67.

Kaur S., Rani S., Mahajan R.K., Asif M., Gupta V.K., (2015), Synthesis and adsorption properties of mesoporous material for the removal of dye safranin: kinetics, equilibrium, and thermodynamics, *Journal of Industrial Engineering and Chemistry*, **22**, 19-27.

Kudo A., Miseki Y., (2009), Heterogeneous photocatalyst materials for water splitting, *Chemical Society Reviews*, **38**, 253-278.

Khataee A., Soltani R.D., Karimi A., Joo S.W., (2015), Sonocatalytic degradation of a textile dye over Gd-doped ZnO nanoparticles synthesized through sonochemical process, *Ultrasonics Sonochemistry*, **23**, 219-230.

Kumar A., Pandey G., (2017), A review on the factors affecting the photocatalytic degradation of hazardous materials, *Material Science and Engineering International Journal*, **1**, 106-114.

Li X., Hou Y., Zhao Q., Wang L., (2011), A general, one-step and template-free synthesis of sphere-like zinc ferrite nanostructures with enhanced photocatalytic activity for dye degradation, *Journal of Colloid Interface Science*, **358**, 102-108.

Mamba G., Mamo M.A., Mbianda X.Y., Mishra A.K., (2014), Nd, N, S-TiO_2 decorated on reduced graphene oxide for a visible light active photocatalyst for dye degradation: Comparison to its MWCNT/Nd, N, S-TiO_2 analogue, *Industrial and Engineering and Chemical Research*, **53**, 14329-14338.

Mengyue Z., Shifu C., Yaowu T., (1995), Photo catalytic degradation of organophosphorus pesticides using thin films of TiO_2, *Journal of Chemical Technology and Biotechnology*, **64**, 339-344.

Nagaraju G., Shivaraju G.C., Banuprakash G., Rangappa D., (2017), Photocatalytic activity of ZnO nanoparticles: synthesis via solution combustion method, *Materials Today: Proceedings*, **4**, 11700-11705.

Perumal S.L., Hemalatha P., Alagara M., Pandiyaraj K.N., (2015), Investigation of structural, optical and photocatalytic properties of Sr doped Zno nanoparticles, *International Journal of Chemistry and Physical Sciences*, **4**, 1-13.

Pradyast A., Azhariyah A.S., Karamah E.F., Bismo S., (2018), *Preparation of Zinc Oxide Catalyst with Activated Carbon Support for Ozone Decomposition*, IOP Conference Series: Earth and Environmental Science, Volume 105, 2nd international Tropical Renewable Energy Conference, (i-TREC) 2017, 3–4 October 2017, Bali, Indonesia.

Raj K.P., Sadaiyandi K., Kennedy A., Thamizselvi R., (2016), Structural, optical, photoluminescence and photocatalytic assessment of Sr-doped ZnO nanoparticles, *Materials Chemistry and Physics*, **183**, 24-36.

Reddy S.S., Kotaiah B., Reddy N.S.P., (2008), Color pollution control in textile dyeing industry effluents using tannery sludge derived activated carbon, *Bulletin of the Chemical Society of Ethiopia*, **22**, 369-378.

Rekha K., Nirmala M., Nair M.G., Anukaliani A., (2010), Structural, optical, photo catalytic and antibacterial active, *Physica B Condensed Matter*, **405**, 3180-3185.

Reza K.M., Kurny A.S.W., Gulshan F., (2017), Parameters affecting the photocatalytic degradation of dyes using TiO_2: A review, *Applied Water Science*, **7**, 1569-1578.

Saggioro E.M., Oliveira A.S., Pavesi T., Maia C.G., Ferreira L.F.V., Moreira J.C., (2011), Use of titanium dioxide photocatalysis on the remediation of model textile wastewaters containing azo dyes, *Molecules*, **16**, 10370-10386.

Salama A., Mohamed A., Aboamera N.M., Osman T.A., Khattab A., (2018), Photo catalytic degradation of organic dyes using composite nanofibers under UV irradiation, *Applied Nanoscience*, **8**, 155-161.

Salvi S., Lokhande P., Mujawar H., (2016), *Photodegradation of Rhodamine 6G dye by Cd, Sr doped ZnO Photocatalyst, Synthesized by Mechanochemical Method*, Int. Conf. Signal. Process Communication (ICCASP 2016), http://doi.org/10.2991/iccasp-16.2017.8.

Sarkar S., Banerjee A., Halder U., Biswas R., Bandopadhyay R., (2017), Degradation of synthetic azo dyes of textile industry: a sustainable approach using microbial enzymes, *Water Conservation Science and Engineering*, **2**, 121-131.

Sarkheil H., Noormohammadi F., Rezaei A.R., Borujeni M.K., (2014), *Dye pollution Removal from Mining and Industrial Wastewaters Using Chitosan Nanoparticles*, Int. Conf. on Agriculture, Environment and Biological Sciences (ICFAE'14).

Shanthi S.I., Poovaragan S., Arularasu M.V., Nithy S., Sundaram R., Magdalane C.M., Maaza M., (2018), Optical, magnetic and photocatalytic activity studies of Li, Mg and Sr doped and un doped zinc oxide nanoparticles, *Journal of Nanoscience and Nanotechnology*, **18**, 5441-5447.

Viswanathan B., (2018), Photocatalytic degradation of dyes: An overview, *Current Catalysis*, **7**, 99-121.

Wang J., Chen R., Xiang L., Komarneni S., (2018), Synthesis, properties and applications of ZnO nanomaterials with oxygen vacancies: A review, *Ceramic International*, **44**, 7357-7377.

Xiong G., Pal U., Serrano J.G., Ucer K.B., Williams R.T., (2006), Photoluminescence and FTIR study of ZnO nanoparticles: the impurity and defect perspective, *Physica Status Solidi C*, **3**, 3577-3581.

Yaseen D.A., Scholz M., (2018), Treatment of synthetic textile wastewater containing dye mixtures with microcosms, *Environmental Science and Pollution Research*, **25**, 1980-1997.

Yousefi R., Jamali-Sheini F., Cheraghizade M., Khosravi-Gandomani S., Sáaedi A., Huang N.M., Azarang M., (2015), Enhanced visible-light photocatalytic activity of strontium-doped zinc oxide nanoparticles, *Material Science and Semiconductor Processing*, **32**, 152-159.

Zhang F., Zhao J., Shan T., Hidaka H., Pelizzetti E., Serpone N., (1998), TiO_2 assisted photo degradation of dye pollutants: II. Adsorption and degradation kinetics of eosin in TiO_2 dispersions under visible light irradiation, *Applied Catalysis B-Environmental*, **15**, 147-156.